Journal of Alloys and Compounds 495 (2010) 1–6

Contents lists available at ScienceDirect

Journal of Alloys and Compounds

journal homepage: www.elsevier.com/locate/jallcom

How the substitution of Zn for Cu destroys superconductivity in YBCO system?

Rishi Kumar Singhal*

Department of Physics, University of Rajasthan, Jaipur 302004, India

ARTICLE INFO

Article history:
Received 28 November 2009
Received in revised form 21 January 2010
Accepted 21 January 2010
Available online 1 February 2010

PACS:
74.25.Jb
74.72.Bk

Keywords:
High T_c superconductors
Magnetic pair breaking
EXAFS
Photoemission

ABSTRACT

Understanding the mechanism of suppression of superconductivity in perovskite cuprates is as important as to discover the cause of its evolution. Substituting Zn for Cu is known to rapidly suppress the superconductivity in these perovskites but the mechanism is still not understood. To throw some light on this, polycrystalline $YBa_2(Cu_{1-x}Zn_x)_3O_{7-\delta}$ samples ($x = 0.0$–0.06) were synthesized and investigated using X-ray diffraction, titration, resistivity, magnetization, X-ray absorption and photoemission measurements. Results show that their oxygen stoichiometry (δ) changes on Zn substitution affect their normal state resistivity as well as their T_c. However, the observed changes cannot be accounted for solely on the basis of changes in δ. Zn cation is found to act as strong scattering centre in the lattice that causes local lattice distortion (LLD). It also induces local magnetic moment as evidenced from our magnetization results. It is concluded that a combination of $\Delta\delta$, LLD and magnetic pair breaking effect is responsible for the observed rapid suppression of superconductivity.

1. Introduction

The $YBa_2Cu_3O_7$ system, unlike the other high T_c perovskite superconductors, has a unique feature in that it has two non-equivalent Cu sites viz., the linear-chain Cu(1) in the O(1)–Cu(1)–O(1) units and the planar Cu(2) in the CuO_2 sheets containing O(2) and O(3). The CuO_2 plane is sometimes referred to as the superconducting plane: any modification in this plane strongly influences the electronic structure and the density and mobility of the charge carriers [1]. A large number of studies have therefore been carried out substituting various cations for Cu as well as Y and Ba and these have yielded useful information about the lattice and electronic structure of the systems [1–6].

Substitution of Y by various 4f cations including the magnetic Gd cation, Ce and Tb in the YBCO(123) system has made little difference to its T_c [7,8]. Pr, however, tends to destroy its superconductivity and for this reason it has received a great deal of attention [9,10]. On the other hand, the substitution at the Cu site always tends to destroy superconductivity, no matter what the substituting cations are. Cations like Ga, Fe, Co and Al tend to preferentially occupy the Cu(1) chain site and lead to the localization of carriers and weakening of the Cu–O chains as carrier reservoir. As a result, the hole-carriers cannot easily transfer to the CuO_2 planes. The pairing and transportation of carriers are thus affected indirectly, and the superconductivity gets suppressed albeit slowly [1,6,11]. Mg ion, when doped, is known to occupy the Cu(1) chain as well as the Cu(2) sites leading to a higher rate of T_c depression [12]. Other cations like Ni and Zn are said to primarily occupy the Cu(2) sites and hence are more detrimental to superconductivity. However, there is a great deal of difference in the rate of T_c depression in the two cases. It is much less in case of Ni [1,6]. However, there is some difference of opinion about the substitutional site of Zn. While some earlier reports [13,14] claim that Zn goes to both the Cu(1) and the Cu(2) sites, later ones [1,15] show that it prefers the Cu(2) site.

The introduction of magnetic ions in the lattice, as per the Abrikosov–Gor'kov (A–G) pair breaking theory [16], leads to a rapid decrease of T_c with increase in the concentration of the magnetic ions due to the interaction of magnetic impurities with the conduction electrons breaking the time-reversal symmetry of the Cooper-pairs [16]. Doping of the magnetic ions like Fe, Co and Ni in the YBCO at the Cu sites induces a magnetic moment and magnetic pair breaking [1]. Introducing the magnetic ion Mn at the Mg site in the MgB_2 also induces a local magnetic moment and the pair breaking effect [17]. Even in the YNi_2B_2C system wherein magnetism can coexist with superconductivity, when magnetic Ho ion is substituted at the Y site, the T_c decreases [18]. In all the above cases the magnetic impurities appear to act as effective magnetic scattering centres and hence magnetic pair-breakers.

However, the most dramatic effect in YBCO is observed on substituting the non-magnetic Zn ions for Cu resulting in a rapid suppression of T_c—only 6% of Zn is enough to fully spoil the superconductivity. Observation of specific EPR and NMR resonances has shown that the Curie term in the bulk susceptibility of Zn-doped sample [19] is due to a magnetic moment induced on the

* Tel.: +91 141 2545931.
E-mail address: singhal46@yahoo.co.in.

0925-8388/$ – see front matter © 2010 Elsevier B.V. All rights reserved.
doi:10.1016/j.jallcom.2010.01.106

Cu sites around Zn [20–22]. Furthermore, the broadening of ^{63}Cu [23,24] and ^{17}O NMR lines [25] in YBCO reveals a distribution of moment magnitudes, attributed to a spatially inhomogeneous spin polarization extending over several lattice sites around Zn. Zn doping also has drastic effects on spin dynamics: low energy anti-ferromagnetic (AF) fluctuations probed by neutron scattering are enhanced [26] and spin freezing eventually occurs [27,28]. Nevertheless, a clear understanding of these effects, particularly the origin of the magnetic moment by non-magnetic Zn, remains elusive.

In this article, we report the results of Zn doping in the YBCO (123) system obtained from: Zn K-edge X-ray absorption near edge structure (XANES) and extended X-ray absorption fine structure (EXAFS), X-ray photoemission spectroscopy (XPS), induced magnetization by VSM, oxygen stoichiometry by titration in addition to standard characterization by XRD, resistivity and ac susceptibility.

2. Materials and measurements

Polycrystalline samples of $YBa_2(Cu_{1-x}Zn_x)_3O_{7-\delta}$ for $x = 0.0$, 0.02, 0.04 and 0.06 were prepared by usual solid-state reaction technique using a microprocessor controlled furnace (Linn, Germany). Appropriate molar quantities of high purity starting oxides Y_2O_3 (Wako Pure Chemical Industries Ltd., 99.99%), $BaCO_3$ (John Baker Inc. USA, 99.99%), CuO (Aldrich 99.9999%) and ZnO (Aldrich, 99.99%) were mixed and heated thrice at 975 °C for 24, 16 and 16 h respectively, with several intermediate grindings to ensure perfect homogeneity and complete the solid-state reaction. The resulting powders were reground and pressed into pellets. The pellets were sintered in flowing oxygen at 990 °C for 12 h followed by slow cooling (~1 °C/min) to 450 °C. They were kept at ~450 °C for ~72 h in flowing O_2 and then gradually cooled to room temperature. The reason for annealing in O_2 is to regain the oxygen that was lost during annealing at 950 °C in view of the evidences that the oxygen intake is optimum in temperature range 400–450 °C.

The XRD patterns were recorded using Philips 1840 powder diffractometer with Fe K_α radiation to check the phase purity and estimate the cell parameters. Four-probe dc-resistivity measurements were carried out using an APD Cryogenics, Inc. Superconductor Characterization Cryostat and a closed cycle Displex CS202 refrigerator for the temperature range 300–20 K. The magnetic susceptibility was measured from 100 K down to 4 K using superconducting quantum interference device (SQUID) magnetometer at CBPF, Brazil. Iodometric titrations were carried out to estimate the oxygen content of the samples [29].

The Zn *2p* and O *1s* core level photoemission spectra were measured using X-ray photoelectron spectrometer at UGC-DAE-CSR, Indore, India. The XPS is a surface sensitive technique; therefore, all the spectra were recorded only after ensuring a clean sample surface. The pellets were scraped uniformly until the feature coming from carbon contamination of the surface (C *1s* peak) got minimized. Sputtering was avoided due to fear of change of surface composition as it may cause differential removal of the light elements from the surface. The vacuum in the chamber was kept at $\sim 4.4 \times 10^{-10}$ Torr, hence, the cleanliness of the samples was conserved during the experiment. No shift was observed due to charging of the samples. The carbon correction was applied to all the spectra, i.e. all the binding energies were corrected with reference to the carbon *1s* line at 284.6 eV.

The X-ray absorption measurements were performed at beamline I811, MAX-lab synchrotron source, Lund Sweden [30]. The flux on the sample was $\sim 10^{12}$ photons/s for a 1 mm diameter beam spot on the sample. The detection was carried out in fluorescence mode using an energy dispersive solid-state detector [31]. The EXAFS data analysis was performed using ATOM 3.0, FEFF 8.0 and UWXAFS 3.0 software packages [32–34]. The absorption edge was determined by the first derivative of first rise at the X-ray absorption spectrum after self-absorption correction (SAC) and base line subtraction. SAC is essential for spectra measured in the FY mode [35–38]. The isolated EXAFS was normalized to the edge step and converted to wave number scale by AUTOBK program. The Fourier transform was performed on k^3-weighted EXAFS oscillations using Hanning windowsills by FEFFIT25 program. FEFFIT25 combines and modifies the EXAFS from a set of feffnnnn.dat files to the best-fit experimental $\chi(k)$ data. The fit was performed on data in K- and R-spaces.

The field dependent magnetization measurements (M–H curves) for all these samples were performed at 300 K using a PARC vibrating sample magnetometer Model 155 [39].

3. Experimental results

3.1. XRD, resistivity, susceptibility and oxygen stoichiometry results

The XRD patterns for $YBa_2(Cu_{1-x}Zn_x)_3O_{7-\delta}$ samples with $x = 0.00$, 0.02, 0.04 and 0.06 (Fig. 1) show a single-phase orthorhombic structure for all the compositions with no detectable impurity phase [40]. Susceptibility and resistivity measurements (Fig. 2) show a good superconducting diamagnetic Meissner volume fraction. Table 1 lists the lattice parameters, the orthorhombicity $\{100 \times (b-a)/(b+a)\}$, the T_c values and the oxygen content in the samples. The orthorhombicity value appears to remain more or less unaffected by Zn substitution. A transition to the non-superconducting tetragonal phase is characterized by a loss in orthorhombicity and hence the rearrangement of O(1) and the O(5) sites [41,42]. In other words, the Zn doping does not seem to affect the linear Cu(1)–O(1) chain and may be justifiably assumed to exclusively go to CuO_2 planes. We would revert to this point later.

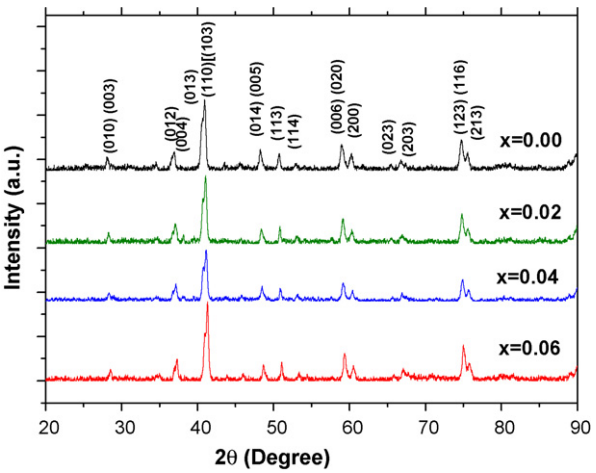

Fig. 1. XRD pattern for the $YBa_2(Cu_{1-x}Zn_x)_3O_{7-\delta}$ system.

The oxygen stoichiometry data (Table 1) shows that the oxygen content progressively decreases with increase in Zn concentration, though slightly. Such a decrease is in conformity with earlier reports [43]. Turning attention to resistivity data one can see the well-established rapid decrease of the T_c with Zn concentration, the superconductivity getting suppressed for ~6% Zn concentration. Furthermore, the normal state resistivity also increases appreciably with increasing Zn content (Fig. 2). This could be at least in part ascribed to the depletion in the oxygen content observed on Zn doping (Table 1). But, there has to be another factor contributing

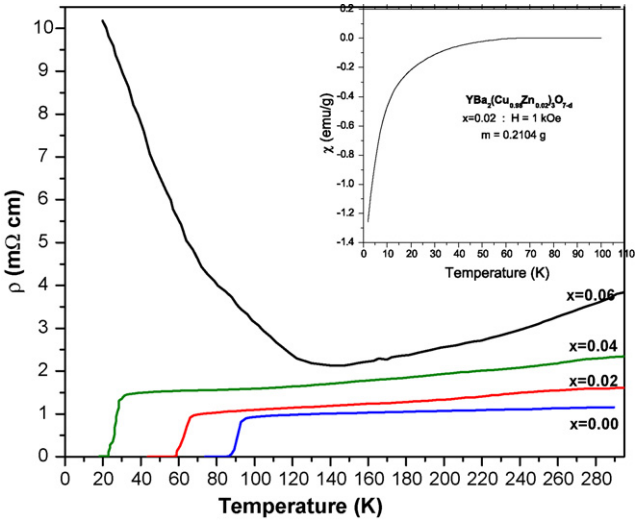

Fig. 2. Resistivity vs. temperature for $YBa_2(Cu_{1-x}Zn_x)_3O_{7-\delta}$ samples and susceptibility for $x = 0.02$ in inset.

Table 1
Cell parameters, T_c values and orthorhombicity for $YBa_2(Cu_{1-x}Zn_x)_3O_{7-\delta}$ samples. Oxygen content estimated from wet titration and the oxygen contents, relative to undoped sample, estimated from O *1s* XPS data are also given.

x	T_c (K) ±0.02	Oxy. cont. (by titration) ±0.02	Rel. oxy. cont. (XPS O *1s* data) ±0.02	a (Å) ±0.001	b (Å) ±0.001	c (Å) ±0.001	Orthorhombicity $100\times(b-a)/(b+a)$
0.00	91.04	6.96	1.00	3.822	3.901	11.675	1.02
0.02	62.15	6.81	0.97	3.819	3.897	11.664	1.01
0.04	26.61	6.79	0.95	3.820	3.899	11.686	1.02
0.06	–	6.74	0.94	3.819	3.894	11.670	0.97

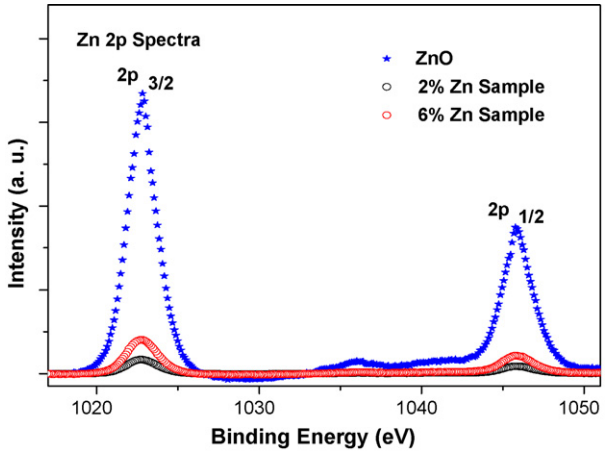

Fig. 3. The Zn $2p_{3/2}$ XPS spectra for ZnO and $YBa_2(Cu_{1-x}Zn_x)_3O_{7-\delta}$ samples ($x=0.02$ and 0.06).

to increase of resistivity. We say so because even our 6% Zn-doped sample has an oxygen count of 6.74 and hence, were there no other factors involved, ought to yield a value of T_c ~70 K [41,44–47]. The Zn cation may thus be causing local lattice distortion (LLD) and acting as a strong scattering centre in the *ab*-plane in the lattice, an effect that is enhanced since Zn primarily replaces Cu from the in-plane sites [1,15]. This is further borne out from our core level XPS, X-ray absorption and VSM measurements discussed below.

3.2. Zn 2p XPS data

The Zn *2p* XPS spectra for $YBa_2(Cu_{1-x}Zn_x)_3O_{7-\delta}$ for $x=0.02$ and 0.06 are shown in Fig. 3 along with the spectrum for ZnO (reference system for Zn^{2+} state). All three spectra show symmetric single peaks located at 1022.7 and 1045.8 eV corresponding to $2p_{3/2}$ and $2p_{1/2}$, respectively. Single Gaussians were nicely fit to all the spectra (not shown) and no change in peak positions noticed with respect to pure ZnO. The symmetric single peaks rule out the possibility of existence of multiple components of Zn in these samples. The peak positions of Zn $2p_{3/2}$ and Zn $2p_{1/2}$ in all the samples match closely with the standard values of ZnO [48] indicating that Zn atoms are in +2 oxidation state. The intensity under the $2p_{3/2}$, $2p_{1/2}$ peaks is more in 6% Zn-doped sample than the 2% Zn-doped sample, which was usual.

3.3. Oxygen 1s XPS data

Oxygen *1s* spectrum shown in Fig. 4a for $YBa_2(Cu_{1-x}Zn_x)_3O_{7-\delta}$ for $x=0.02$, is asymmetric, indicating that multi-component oxygen species can not be ruled out in the near-surface region of the samples. Three Gaussians were fitted to these spectra to separate out this contribution. The most intense first peak at ~530 eV is due to oxygen *1s* bulk contribution from the oxide samples. Our main interest lies in relative intensity of this feature. However, the high-energy peaks are due to chemisorbed oxygen of the surface hydroxyl, $-CO_3$, absorbed H_2O, absorbed O_2 or mainly due to the surface contamination [49]. The intensities of the first Gaussian (oxygen *1s* peak) are displayed in Fig. 4b for all the samples ($x=0.0$, 0.02, 0.04 and 0.06). The relative oxygen contents, estimated by the ratio of area under these O *1s* Gaussian peaks in different samples divided by the area under this peak of undoped YBCO sample, are shown in Table 1. It is evident that oxygen content decreases progressively with increasing Zn content, in agreement with the titration results.

3.4. XANES results

Fig. 5 shows the background-subtracted and normalized Zn K-absorption edge spectra which resemble the Zn K-edge XANES spectra of ZnO (not shown) measured by Mizoguchi et al. [50] on a ZnO (wurtzite) single crystal, and show all the fine structures observed by them. We have labelled the fine structures in

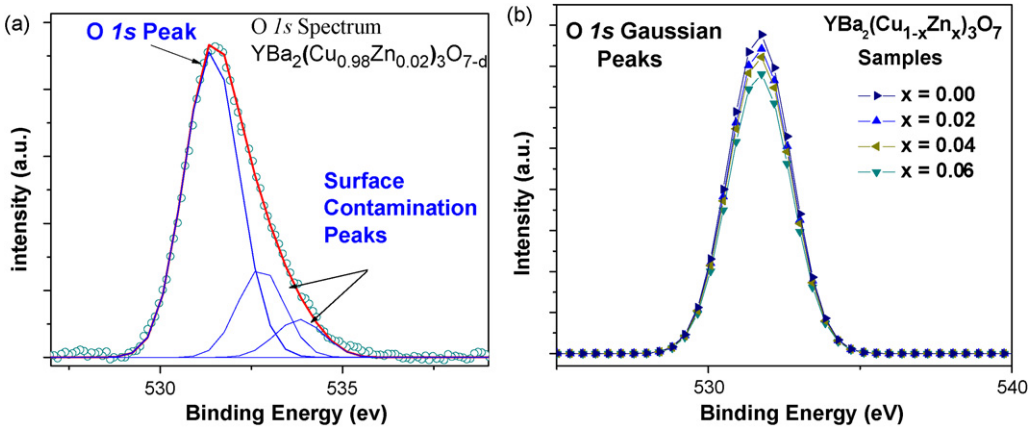

Fig. 4. (a) The O *1s* XPS spectrum, with Gaussian fits for $YBa_2(Cu_{1-x}Zn_x)_3O_{7-\delta}$ ($x=0.02$) and (b). Comparison of the O*1s* Gaussian peaks for $YBa_2(Cu_{1-x}Zn_x)_3O_{7-\delta}$ samples ($x=0.0$, 0.02, 0.04 and 0.06).

Table 2
Values of Zn-O, Zn-Y distances and other structural parameters obtained from EXAFS analysis done for the first four n-n for $YBa_2(Cu_{1-x}Zn_x)_3O_{7-\delta}$ samples.

x (Å)	Zn-O(2)		Zn-O(3)		Zn-O(4)		Zn-Y		Amp. red. factor, S_0^2	D–W factor, σ^2 (Å^2)
	r-eff. (Å)	Deg. (n1)	r-eff. (Å)	Deg. (n2)	r-eff. (Å)	Deg. (n3)	r-eff. (Å)	Deg. (n4)		
0.02	1.9806	2	2.0159	2	2.3769	1	3.2917	4	0.79	0.0012
0.06	1.9780	2	2.0132	2	2.3738	1	3.2874	4	0.81	0.0011

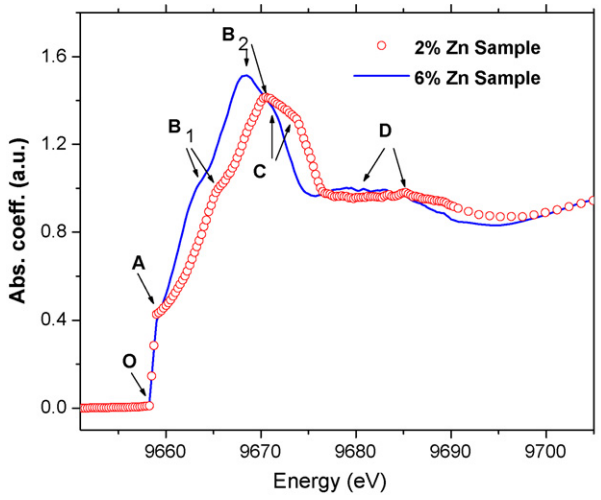

Fig. 5. XANES spectra for $YBa_2(Cu_{1-x}Zn_x)_3O_{7-\delta}$ samples (x = 0.02 and 0.06).

our spectra in the same way as Mizoguchi et al. [50] to facilitate comparison with their spectra. However, the initial absorption rise part in our spectra, measured with an interval of 0.25 eV, is rather rapid. Further, comparing the 2% and 6% spectra (Fig. 5) the initial absorption rise parts completely overlap each other implying thereby that there is no shift in the absorption edge when the Zn content is varied. However, the peaks/shoulders B_1, B_2, C and D shift to lower energy side by about 3 eV as the Zn content increases from 2% to 6%. Mizoguchi et al. [50] have, from their polarized XANES measurements and orthogonalised linear combinations of atomic orbitals calculations, ascribed the origin of the structures B_1 and C to the $E//c$ symmetry and the B_2 to the $E//ab$ symmetry (E is the electric field vector). Since there is no shift in the absorption edge as such, the observed shift of the other structures cannot be ascribed to changes in the electronic structure that may be caused by Zn doping. Instead, these strongly point to the Zn dopant ion causing LLD that may, in turn, result in the lowering of the energy of the 4p-symmetric states.

3.5. EXAFS results

Zn K-absorption edge EXAFS spectra were recorded for two of these samples, i.e. x = 0.02 and 0.06. Fig. 6(a) and (b) represents the k^3-weighted experimental and the fitted Fourier transformed $\chi(k)$ spectra, for one of these samples (x = 0.06), both in the K-space and R-space. The EXAFS fitting has been done for the first four near-neighbours from 0.9 to 3.25 Å as these are the ones that are of utmost interest. The fits in all the cases were quite good. The Zn–O distances and the co-ordination number for each shell and other fit parameters such as the Debye–Waller factor σ^2 and the amplitude reduction factor S_0^2 obtained from the fits are given in the Table 2. It shows that all Zn–O distances, in-plane and along the c-axis, as well as the Zn–Y distances tend to decrease with increase in Zn concentration. This is rather surprising as the ionic radius of Zn^{2+} (ionic radii 0.74 Å) is slightly larger than that of Cu^{2+} (ionic radii 0.77 Å) [51]. From the EXAFS fitting results of the n-n distances we see that the fourth near-neighbour to Zn turns out to be the Yttrium ion with a degeneracy of 4 which implies that the Zn is occupying the Cu(2) site in the Cu-O_2 plane. If it were going to the Cu–O chain then the fourth n-n would be Ba and not Y [1,52–55]. Considering our EXAFS data and its aforementioned implications it is quite reasonable to conclude that the LLD resulting from Zn doping, in part is due to the Zn ion acting as a strong in-plane scattering centre and, in part is due to the loss in oxygen content as Zn is substituted for Cu.

4. Discussion

In order to further appreciate the implication of such LLD we also measured the M–H curves for these samples (Fig. 7). The results clearly showed a systematic increase in the susceptibility with the increase in Zn concentration. The observed LLD and the increase in susceptibility of the samples may thus be inter-related, the latter being a consequence of the former. Mahajan et al. [21] have also demonstrated that the local moments, responsible for the enhanced susceptibility, do not result from holes trapped on the n-n oxygen orbitals, but rather from the modifications of the magnetic properties of the neighbouring Cu holes. They have clearly shown that

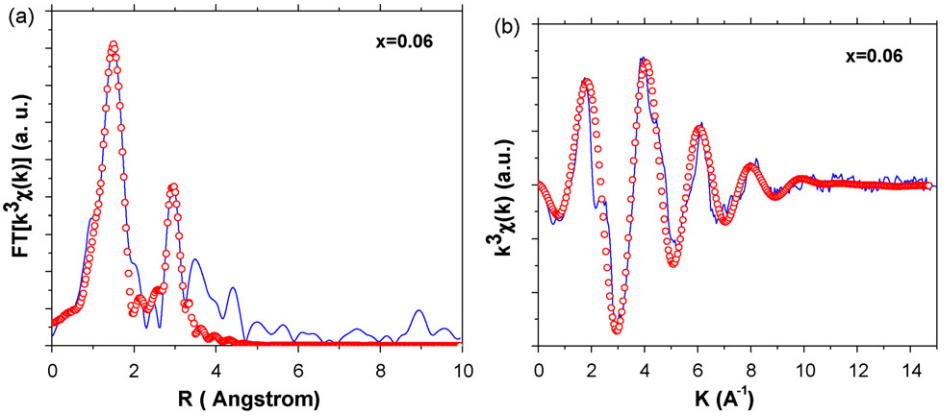

Fig. 6. (a and b) The k^3-weighted Fourier transformed spectra {experimental (—) and fitted (○)} in K- and R-spaces, respectively, for $YBa_2(Cu_{0.94}Zn_{0.06})_3O_{7-\delta}$ sample.

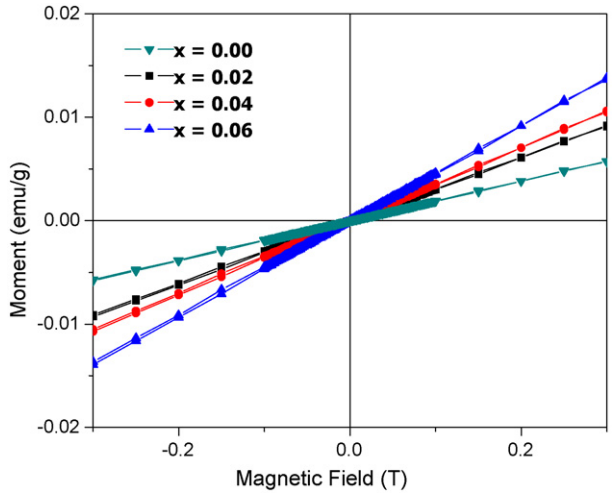

Fig. 7. Magnetization curves for $YBa_2(Cu_{1-x}Zn_x)_3O_{7-\delta}$ samples at 300 K.

the exchange coupling J_{eff} between the local moments and the Cu holes has the same order of magnitude as that between the Cu spins of the pure material [19]. Low temperature *M–H* curves measured by them using SQUID also show a strong and anomalous increase in magnetization and an increase in anisotropy in the single crystals of the Zn-doped YBCO system [56]. Various other experimental techniques like Cu NMR, Y NMR, SQUID and Muon Spin resonance [21,57–60] also show that the Zn doping causes magnetic modifications by inducing a local magnetic moment on its neighbours in the YBCO system. Apart from these, there are recent reports that the Al in LSCO [61], Mn in MgB_2 [17], Ho in $Y_{1-x}Ho_xNi_2B_2C$ [18] also induce such local magnetic moments and enhance the Abrikosov–Gor'kov pair breaking [16]. Thus, our results also support magnetic pair breaking as the dominant cause for the suppression of superconductivity on Zn doping.

However, it is pertinent to ask if the decrease in T_c is solely due to the magnetic pair breaking. Our samples do show a progressive decrease in oxygen content with increase in Zn content, which, in turn, would lead to a depletion of the itinerant hole and hence contribute to lowering of the T_c. But, this alone cannot account for the rapid fall in the T_c for, as discussed earlier, it should show a $T_c \sim 70$ K. Yang et al. [1] also state that oxygen hole-density alone is not responsible for the depression of T_c in the Zn-doped YBCO-123 system.

Turning attention to the observed normal state resistivity in our samples (Fig. 2) and comparing these with the data of Cava et al. [45] on the pristine YBCO with different oxygen content (oxygen based phase diagram), we find that the normal state resistivity in our case is higher than the corresponding case (equal oxygen content) in Cava et al.'s data [45]. It is well known that the presence of defects and impurities lead to enhanced scattering of charge carriers and hence the Zn defect centres (LLD) must be responsible for it in our case. Furthermore, Panagopoulos et al. [62] have reported that the penetration depth decreases and Tomimoto et al. [63] claim an increase in the coherence length by the increase of the Zn concentration in the YBCO (123) system. Both these results point to creation of some type of distorted scattering centres in the system upon Zn doping that might scatter the holes pairs which would cause the pair breaking and hence the suppression of the superconductivity. Segawa et al. [64] have referred to the Zn impurity as the point-like defects. Such distorted centres would also scatter unpaired holes leading to increase in normal state resistivity.

5. Conclusion

In conclusion, we have studied experimentally the transport and magnetic properties, crystal and electronic structure of $YBa_2(Cu_{1-x}Zn_x)_3O_{7-\delta}$ system. We found that Zn cations substituted for Cu all go to occupy the Cu planar site. The substitution leads to a change in oxygen stoichiometry and local lattice distortion with the Zn cation acting as a strong scattering centre and inducing of local magnetic moment that increases with Zn concentration. While the changed oxygen stoichiometry, as shown by our titration and O *1s* core level XPS spectra, does lead to a decrease in the itinerant hole-density and hence the T_c, it is the magnetic pair breaking that plays a main role in suppression of superconductivity, as per the Abrikosov–Gor'kov (A–G) pair breaking theory.

Acknowledgements

Author is thankful to the TWAS, Trieste, Italy for a fellowship. Part of this work was done at IUC-DAE-CSR, Indore, India. Author is grateful to Prof. K.B. Garg, Univ. of Rajasthan, India for providing the EXAFS spectra measured at MAX-lab, Sweden.

References

[1] C.Y. Yang, A.R. Moodenbaush, Y.L. Wang, Y. Xu, S.M. Heald, D.O. Welch, M. Suenaga, D.A. Fischer, J.E. Penner-Hahn, Phys. Rev. B 42 (1990) 2231–2241.
[2] T. Harada, K. Yoshida, Physica C 391 (2003) 1–7.
[3] H.A. Blackstead, J.D. Dow, Phys. Rev. B 51 (1995) 11830–11837.
[4] H.A. Blackstead, J.D. Dow, Solid State Commun. 115 (2000) 137–140.
[5] S. Lei, H. Yunsong, J. Yunbo, L. Xianming, Z. Guien, Z. Yuheng, J. Phys.: Condens. Mater. 10 (1998) 7015–7024.
[6] Y.X. Zhou, S. Scruggs, K. Salama, Supercond. Sci. Technol. 19 (2006) S556–S561.
[7] G. Cao, R.J. Kennedy, J.W. O'Reilly, J.E. Crow, P. Pernambuco-Wise, S.T. Ting, Physica B: Condens. Matter 186–188 (1993) 1022–1026.
[8] C.R. Fincher Jr., G.B. Blanchet, Phys. Rev. Lett. 67 (1991) 2902–2905.
[9] S.K. Gaur, R.K. Singhal, K.B. Garg, T. Shripathi, U.P. Deshpande, E.M. Bittar, P.G. Pagliuso, Elisa Saitovitch, J. Phys.: Condens. Mater. 19 (2007) 326201–326212.
[10] M.R. Mohammadizadeh, M. Akhavan, Phys. Rev. B 68 (2003) 104516–1045228.
[11] P. Li, J. Zhang, G. Cao, C. Jing, S. Cao, Phys. Rev. B 69 (2004) 224517–224523.
[12] V.N. Vieira, P. Pureur, J. Schaf, Phys. Rev. B 66 (2002) 224506–224516.
[13] T. Kajitani, K. Kusaba, M. Kikuchi, Y. Syono, M. Hirabayashi, Jpn. J. Appl. Phys. 27 (1988) L354–L357.
[14] G. Roth, P. Adelmann, R. Ahrens, B. Blank, H. Borkle, F. Gompf, G. Heger, M. Herview, M. Nindle, B. Obst, J. Pannetier, B. Renker, H. Rietschel, B. Rudolf, H. Wuhl, Physica C 162–164 (1989) 518–519.
[15] K. Isida, Y. Kitaoka, T. Yositomi, N. Ogata, T. Kamino, K. Asayama, Physica C 179 (1991) 29–38.
[16] A.A. Abrikosov, L.P. Gor'kov, Sov. Phys. JETP 12 (1961) 1243 [A.A. Abrikosov and L.P. Gor'kov, ZETF 39 (1960), 1781].
[17] K. Rogacki, B. Batlogg, J. Karpinski, N.D. Zhigadlo, G. Schuck, S.M. Kazakov, P. Wagli, R. Puzniak, A. Wisniewski, F. Carbone, A. Brinkman, D. Van der Marel, Phys. Rev. B 73 (2006) 174520–174527.
[18] S.-R. Zhao, J.-Q. Shen, Z.-A. Xu, H. Takeya, K. Hirata, Chin. Phys. Lett. 23 (4) (2006) 975–977.
[19] P. Mendels, J. Bobroff, G. Collin, H. Alloul, M. Gabay, J.F. Marucco, N. Blanchard, B. Grenier, Europhys. Lett. 46 (1999) 678–684.
[20] A.M. Finkel'stein, V.E. Kataev, E.F. Kukovitskii, G.B. Teitel'baum, Physica C 168 (1990) 370–380.
[21] A.V. Mahajan, H. Alloul, G. Collin, H.-F. Marucco, Phy. Rev. Lett. 77 (1994) 3100–3103.
[22] G.V.M. Williams, J.L. Tallon, R. Meinhold, Phys. Rev. B 52 (1995) R7034–R7037.
[23] R.E. Walstedt, R.F. Bell, L.F. Schneemeyer, J.V. Waszczak, W.W. Warren, R. Dupree, A. Gencten, Phys. Rev. B 48 (1993) 10646–10649.
[24] G.-q. Zheng, T. Odaguchi, Y. Kitaoka, K. Asayama, Y. Kodama, K. Mizuhashi, S. Uchida, Physica C 263 (1996) 367–370.
[25] J. Bobroff, H. Alloul, Y. Yoshinari, A. Keren, P. Mendels, N. Blanchard, G. Collin, J.-F. Marucco, Phys. Rev. Lett. 79 (1997) 2117–2120.
[26] Y. Sidis, P. Bourges, B. Hennion, L.P. Regnault, R. Villeneuve, G. Collin, J.-F. Marucco, Phys. Rev. B 53 (1996) 6811–6818.
[27] P. Mendels, H. Alloul, J.H. Brewer, J.D. Morris, T.L. Duty, S. Johnston, E.J. Ansaldo, G. Collin, J.-F. Marucco, C. Niedermayer, D.R. Noakes, C.E. Stronach, Phys. Rev. B 49 (1994) 10035–10038.
[28] C. Bernhard, Ch Niedermayer, Blasius, G.V.D. Williams, R. De Renzi, C. Bucci, J.L. Tallon, Phys. Rev. B 58 (1998) R8937–R8940.
[29] D.C. Harris, T.A. Hewston, J. Solid State Chem. 69 (1987) 182–185.
[30] T.M. Grehk, P.O. Nilsson, Nucl. Instrum. Methods Phys. Res. A 467–468 (2001) 635–638.
[31] S. Carlson, M. Clausén, L. Gridneva, B. Sommarin, C. Svensson, J. Synchrotron Radiat. 13 (2006) 359–364.

[32] J. Rehr, S.I. Zabinsky, R.C. Albers, Phys. Rev. Lett. 69 (1992) 3397–3400.
[33] A.E. Stern, Phys. Rev. B 48 (1993) 9825–9827.
[34] B. Raval, M. Newville, J.O. Cross, C.E. Bouldin, Physica B 145 (1995) 208–217.
[35] L. Troger, D. Arvanitis, K. Babershke, Phys. Rev. B 46 (1992) 3283–3289.
[36] M. Merz, N. Nucker, E. Pelligrinm, P. Schweiss, S. Schuppler, Phys. Rev. B 55 (1997) 9160–19160.
[37] C.T. Chen, L.H. Tjeng, J. Kwo, H.L. Kao, P. Rudolf, F. Sette, R.M. Fleming, Phys. Rev. Lett. 68 (1992) 2543–2546.
[38] Y.U. Idzerda, C.T. Chen, H.J. Lin, G. Meigs, G.H. Hoand, C. Kao, Nucl. Instrum. Methods Phys. Res. A 347 (1994) 134–141.
[39] S.K. Gaur, Ph.D. Thesis, submitted to University of Rajasthan, Jaipur, India, 2009.
[40] B. Gogia, R.D. Tarey, D.K. Pandya, S.C. Kashyap, K.L. Chopra, in: A.K. Gupta, S.K. Joshi, C.N.R. Rao (Eds.), Proc. Workshop on High Temperature Superconductivity, Srinagar, India, 1988, pp. 267–271.
[41] J.D. Jorgensen, M.A. Beno, D.J. Hinks, L. Soderholm, K.J. Volin, R.L. Hitterman, J.D. Grace, I.K. Schuller, C.U. Segre, K. Zhang, M.S. Kleefisch, Phys. Rev. B 36 (1987) 3608–3616.
[42] J.D. Jorgensen, B.W. Veal, W.K. Kwox, C.W. Crabtree, A. Umezawa, L.J. Novoski, A.P. Paulikas, Phys. Rev. B 36 (1987) 5731–5734.
[43] T.V. Ramakrishnan, C.N.R. Rao, J. Phys. Chem. 93 (1989) 4414–4422.
[44] A. Kapitulnik, M.R. Beasley, C. Castellani, C. Di Castro, Phys. Rev. B 37 (1988) 537–540.
[45] R.J. Cava, B. Batlogg, C.H. Chen, E.A. Rietman, S.M. Zahurak, D. Werder, Phys. Rev. B 36 (1987) 5719–5722.
[46] Y. Ando, A.N. Lavrov, K. Segava, Phys. Rev. Lett. 83 (1999) 2813–2816.
[47] K. Segawa, Y. Ando, Phys. Rev. Lett. 86 (2001) 4907–4910.
[48] C.D. Wagner, W.M. Riggs, L.E. Davis, J.F. Moulder, G.E. Muilenberg, Handbook of X-ray Photoelectron Spectroscopy, Perkin Elmer, Eden Prairie, 1979, p. 80 and 84.
[49] R.K. Singhal, M.S. Dhawan, S.K. Gaur, S.N. Dolia, Sudhish Kumar, T. Shripathi, U.P. Deshpande, Y.T. Xing, E. Saitovitch, K.B. Garg, J. Alloys Compd. 477 (2009) 379–385.
[50] T. Mizoguchi, I. Tanaka, S. Yoshioka, M. Kunisu, T. Yamamoto, W.Y. Ching, Phys. Rev. B 70 (2004) 045103–045112.
[51] R.D. Shanon, Acta Crystallogr. A 32 (1976) 751–767.
[52] F. Bridges, L. Gouguang, J.B. Boyce, T. Claeson, Phys. Rev. B 48 (1993) 1266–1275.
[53] Y. Zhao, H.K. Liu, J.R. Li, G. Yang, S.X. Dou, Physica C 190–189 (1991) 753–754.
[54] Y. Saito, T. Noji, A. Endo, N. Higuchi, K. Fujimoto, T. Oikawa, A. Hattori, K. Fukuse, Physica B+C 148 (1987) 336–338.
[55] R. Dupree, A. Gencten, D.McK. Paul, Physica C 193 (1992) 81–89.
[56] K. Takita, S. Kuruda, M. Hussain, Physica C 297 (1998) 176–184.
[57] J. Bobroff, H. Alloul, Y. Yoshinari, Y. Mendels, N. Blanchard, G. Collin, J.-F. Marucco, Physica C 282–287 (1997) 1389–1390.
[58] M.H. Julien, T. Feher, M. Horvatic, C. Berthier, O.N. Bakharev, P. Segransan, G. Collin, H.-F. Maruccu, Phys. Rev. Lett. 84 (2000) 3422–3425.
[59] S. Ouazi, J. Bobroff, H. Alloul, W.A. MacFarlane, Phys. Rev. B 70 (2004) 104515–104522.
[60] M.-H. Julien, Y. Tokunaga, T. Feher, M. Horvatic, C. Berthier, Phys. Rev. B 71 (2005) 176501–176504.
[61] K. Ishida, Y. Kitaoka, K. Yamazoe, K. Asayama, Y. Yamada, Phys. Rev. Lett. 76 (1996) 531–534.
[62] C. Panagopoulos, J.R. Cooper, N. Athanassopoulou, J. Chrosch, Phys. Rev. B 54 (1996) R12721–R12724.
[63] K. Tomimoto, I. Terasaki, A.I. Rykov, T. Mimura, S. Tajima, Phys. Rev. B 60 (1999) 114–117.
[64] K. Segawa, Y. Ando, Phys. Rev. B 59 (1999) R3948–R3951.